IEEE Photonics Journal
An IEEE Photonics Society Publication

Open Access

Optical Implementation of Butler Matrix for Hardware-Efficient Multiuser Beamforming

Volume 10, Number 2, April 2018

Huiyuan Liu
Xiang Liu
Frank Effenberger
Naresh Chand
Xiaofeng Qi
Guifang Li

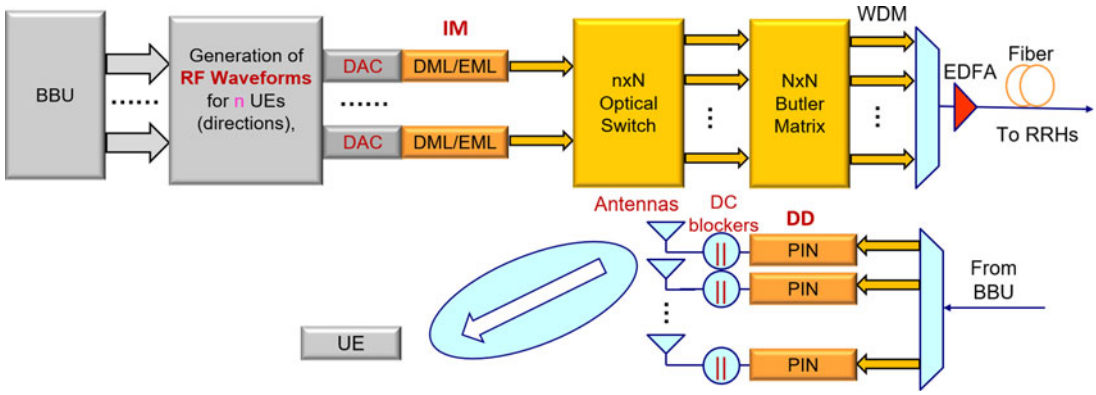

DOI: 10.1109/JPHOT.2018.2805875
1943-0655 © 2018 IEEE

IEEE photonics SOCIETY

IEEE

Optical Implementation of Butler Matrix for Hardware-Efficient Multiuser Beamforming

Huiyuan Liu,[1,2] **Xiang Liu**,[1] **Frank Effenberger**,[1] **Naresh Chand**,[1] **Xiaofeng Qi**,[1] **and Guifang Li**[2]

[1]Futurewei Technologies, Huawei R&D USA, Bridgewater, NJ 08807 USA
[2]CREOL, College of Optics and Photonics, University of Central Florida, Orlando, FL 32816 USA

DOI:10.1109/JPHOT.2018.2805875

Manuscript received February 2, 2018; accepted February 8, 2018. Date of publication February 19, 2018; date of current version March 2, 2018. Corresponding author: Huiyuan Liu (e-mail: huiyuan@knights.ucf.edu).

Abstract: Phased antenna arrays have been used extensively for massive MIMO-based multiuser beamforming to improve both the throughput and power efficiency of wireless communication systems. Beamforming can be realized by the Butler matrix, which has been demonstrated in the electric domain. With wireless systems migration toward simplified remote radio units through radio-over-fiber and sharing of signal processing functions located in the central office, it is desirable to implement this beamforming technique in the optical domain. In this paper, we propose an optical implementation of the Butler matrix using purely passive optical components such as directional couplers and delay lines. With the additional use of optical routing elements, the number of signal streams connected to the baseband unit equals the number of the actual users rather than the number of antenna elements, thereby achieving hardware efficiency for multiuser beamforming. Moreover, the proposed optical Butler matrix acts on the optical intensity rather than the optical field, and therefore, low-cost intensity-modulation direct-detection (IMDD) optical transceivers can be used. A proof-of-concept experiment is conducted to demonstrate the optical 2 $\times$ 2 Butler matrix. Scaling the optical Butler matrix to high port counts is also discussed.

Index Terms: Microwave photonics, optical fibers, phased arrays, beam steering, Butler matrices, optical interconnections.

1. Introduction

Internet traffic has been growing exponentially due to bandwidth-demanding services such as video streaming and multiple-device control. Keeping up with the rate of growth of internet capacity necessitates new technological breakthroughs in every aspect of the internet infrastructure. To support future bandwidth-hungry applications on mobile platforms, the 5th generation wireless communication (5G) has become a hot topic in both academic and industrial research [1], [2] as long-term evolution (LTE) system reaches its maturity.

To access broader bandwidth, the millimeter wave (MMW)) band has been proposed for 5G [3], [4]. Because conventional microwave frequencies (from several hundred MHz to a few GHz) are nearly fully occupied, the MMW spectrum occupying the 30–300 GHz range is the logical next step. Due to its short wavelength, MMW signals suffer from high path loss and low diffraction around obstacles.

So MMW systems are naturally more suitable for very-short-distance and indoor transmission. To achieve longer transmission distance and lower power consumption when supporting many users, massive multiple-input-multiple-output (MIMO) beamforming techniques are currently under intense research such as large-scale multiple antenna (LSMA) to improve link reliability, power efficiency and capacity [5]. A beamforming network can steer the transmitting signal to a specific direction to increase the power efficiency. A beamforming network is also capable of multi-user beamforming, which is very important in 5G. Phased antenna arrays (PAAs) that can realize prescribed phase relationships between successive antenna elements have been utilized to achieve beamforming for microwave wireless communication [6], [7]. The number and complexity of the drive signals increase for large-scale antenna arrays.

Recently radio-over-fiber (RoF) PAAs have attracted significant attention due to their small size and weight, low attenuation, large bandwidth, and immunity to electromagnetic interference [8], [9]. More importantly, RoF can move the phase control network to the central office, simplifying base stations. However, usually phase modulation and accurate optical phase manipulation are used in RoF PAAs [10]–[12], rendering these systems complex and unstable. Here, we propose a new RoF PAA driving network in which, only simple intensity modulation on the transmitter side and direct detection on the receiver side are needed. This method is based on the Butler matrix design, which has been extensively used in electrical PAAs [13]. Signals launched into one input port of the Butler matrix is steered in a specific direction for the downlink. For the uplink, as a result of reciprocity, the received wireless signal from a certain direction would appear at the corresponding output port of the Butler matrix. The proposed method therefore can save a lot of RF components, the number of which is related with the user number rather than the antenna number. Several optical Butler matrix networks have been demonstrated in the past; they have smaller size and wider bandwidth compared with electrical Butler matrixes [14]–[16]. However, they always need accurate, complicate optical phase control, and active phase feedback are usually necessary. In this paper we propose a simple photonic-assisted Butler matrix network using low-cost intensity-modulation direct-detection (IMDD). The passive phase control in this network is for RF signal transmitted on the optical carrier, instead of the phase of the optical carrier itself.

The paper is organized as follows. Section 2 introduces the concept of Butler matrix in term of how it works and the mechanism of our proposed RoF Butler matrix. Section 3 provides details of the experimental setup and results. Section 4 presents possible designs for larger-scale RoF Butler matrices and related components. Finally, Section 5 concludes the paper.

2. Optical Implementation of the Butler Matrix for Beamforming

Butler matrix is a square matrix consisting of passive components including 90-degree hybrids and phase shifters. Unlike other beamforming networks, the Butler matrix network doesn't need active phase control for each antenna channel, yielding cost and space savings. A signal launched into an input port is distributed into each output port with a linear phase ramp, steering the output beam into a direction that is determined by the rate of the phase ramp. In the Butler matrix, each input port produces a different rate phase ramp so the number of directions that the Butler matrix can steer into is equal to the number of input ports.

The schematic of a 4×4 electrical Butler matrix is shown in Fig. 1(a), which consists of RF hybrid couplers and phase shifters. Given the scattering matrix of an RF hybrid coupler

$$H = \frac{1}{\sqrt{2}} \begin{bmatrix} 1 & e^{-j90^\circ} \\ e^{-j90^\circ} & 1 \end{bmatrix}, \tag{1}$$

the input-output relationship of the Butler matrix in Fig. 1(a) is

$$E_{Dout} = C * E_{Din} = \begin{bmatrix} E_1 \\ E_2 \\ E_3 \\ E_4 \end{bmatrix} = \frac{1}{4} \begin{bmatrix} e^{-j45^\circ} & e^{-j135^\circ} & e^{-j90^\circ} & e^{-j180^\circ} \\ e^{-j90^\circ} & e^{-j0^\circ} & e^{-j225^\circ} & e^{-j135^\circ} \\ e^{-j135^\circ} & e^{-j225^\circ} & e^{-j0^\circ} & e^{-j90^\circ} \\ e^{-j180^\circ} & e^{-j90^\circ} & e^{-j135^\circ} & e^{-j45^\circ} \end{bmatrix} \begin{bmatrix} E_{1R} \\ E_{2L} \\ E_{2R} \\ E_{1L} \end{bmatrix}. \tag{2}$$

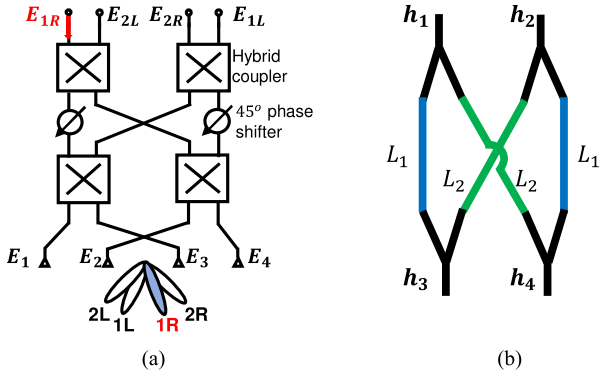

Fig. 1. (a) Schematic of a 4 × 4 electrical Butler matrix. (b) Schematic of a RoF hybrid coupler.

where $E_{D\,\text{out}}$ and $E_{D\,\text{in}}$ are voltages of the output and input RF signals, C is the scattering matrix of the Butler matrix. Linear phase change at the output ports for the signal launched into each input port can be seen from each column of the scattering matrix. The rates of phase ramp corresponding to each input port are -45°, $+135^\circ$, -135°, and $+45^\circ$, respectively. So, the four input ports will be steered to four different directions.

The scattering matrix has a few interesting properties. First, the scattering matrix is identical to a four-point discrete Fourier transform (DFT) matrix. Second, it is a unitary matrix. When the Butler matrix shown in Fig. 1(a) is used as a receiving antenna, the input-output matrix C^T is the transpose of the transmitting matrix. As a result, an incoming beam in the reverse direction of the corresponding transmitting beam will only produce an output at the same port.

In RoF PAAs, the Butler matrix shown in Fig. 1(a) must be implemented for RF signals modulated on an optical carrier, preferably using IMDD. To do so, we need 90-degree hybrids and phase shifters for the IMDD RoF signals. A relative phase shift of $\Delta\phi_{RF}$ for the RoF signal can be realized using optical delay lines, such as waveguides and fibers, of length

$$\Delta L = \frac{\Delta\phi_{RF}}{n_g\,(2\pi f_{RF}/c)}. \tag{3}$$

where n_g is the group index of waveguide, f_{RF} is the frequency of RF signal, c is the speed of light in the vacuum. A 90-degree hybrid coupler for the RoF signal can be realized using 4 1 × 2 passive optical couplers and delay lines as shown in Fig. 1(b), as long as $\Delta L = L_2 - L_1 = 90^\circ/[n_g(2\pi f_{RF}/c)]$.

The beamforming signals produced by the RoF Butler matrix using 90-degree hybrids shown in Fig. 1(b) can be transported to a remote antenna site using optical fibers. The block diagram of such an RoF beamforming system is shown in Fig. 2(a). For each user, the desired RF waveform is generated, and after digital-to-analog conversion (DAC), then modulated onto the intensity of a laser. The $n \times N$ optical switch directs the RoF signal to the desired input port of the $N \times N$ Butler matrix. The output RoF signals from the Butler matrix are transmitted into the antenna section using either a fiber bundle or by using wavelength-division multiplexing (WDM) over O-band in a single fiber. The RF beamforming signals are recovered using direct detection.

The uplink performs the reversed signal transmission as shown in Fig. 2(b). The RF waveform from a user is received by antenna elements. The RF waveforms from these antenna elements having a linear phase ramp are then intensity modulated onto the optical carriers. These RoF signals are transmitted via fibers to the central office. In the ideal case, after propagating through the Butler matrix, the RoF signal from one user will exit out of only one port. The output signal can then be photo-detected and processed in the digital domain after analog-to-digital conversion (ADC). With multi-path interference, MIMO digital signal processing (DSP) is unavoidable. Butler matrix can also reduce the MIMO DSP complexity since it performs demultiplexing.

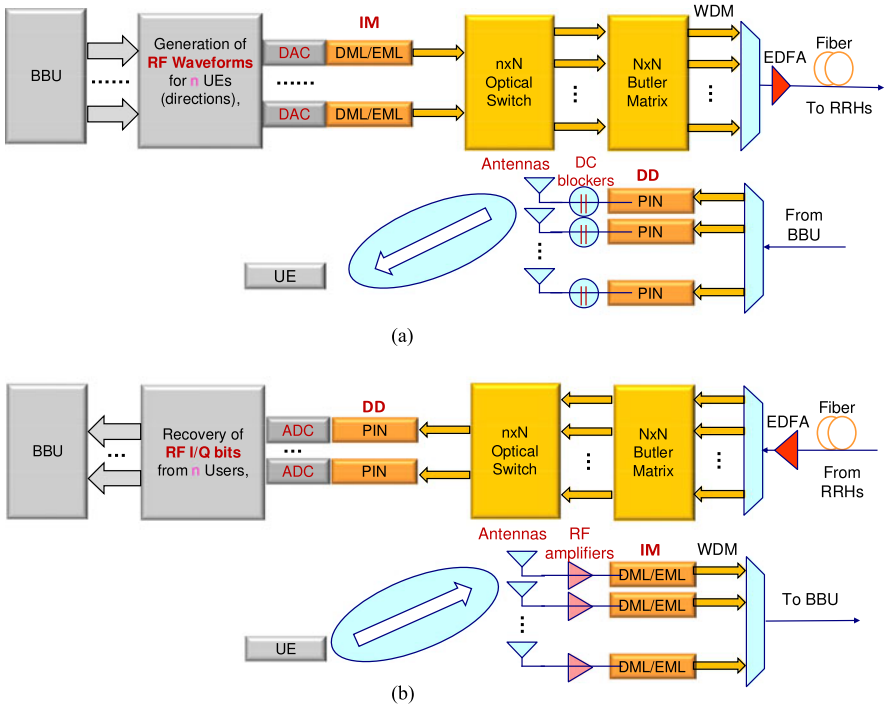

Fig. 2. The block diagram of RoF beamforming network using Butler matrix for (a) downlink and (b) uplink. BBU: baseband unit, DAC: digital-to-analog converter, ADC: analog-to-digital converter, IM: intensity modulation, DML: directly modulated laser, EML: externally modulated laser, WDM: wavelength-division multiplexing, EDFA: erbium-doped fiber amplifier, RRH: remote radio head, DD: direct detection, UE: user equipment.

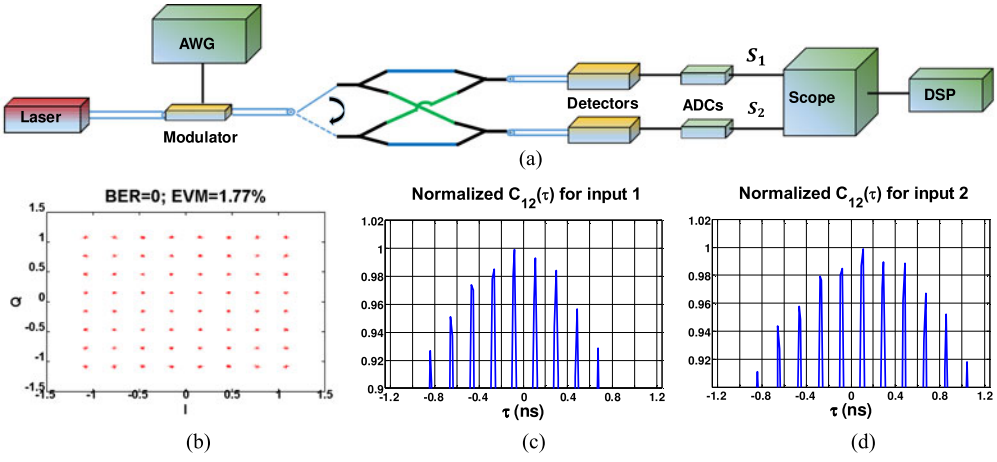

Fig. 3. Downlink demonstration. (a) Experiment setup. AWG: Arbitrary waveform generator, ADC: analog-to-digital converter, Scope: oscilloscope, DSP: digital signal processing. (b) Constellation scheme for 64 QAM. (c)(d) Cross correlations of two outputs for the first and the second input, respectively.

3. Experimental Demonstration of a 2 × 2 Optical Butler Matrix

To demonstrate the feasibility of the Butler matrix, we performed a preliminary experimental demonstration of a 2 × 2 Butler matrix for RoF signals. The experimental setup for the down link is shown in Fig. 3(a). The goal of the downlink demonstration is to verify that, when the RoF signal enters into different input port of the Butler matrix, high-quality microwave signals for driving the transmitting

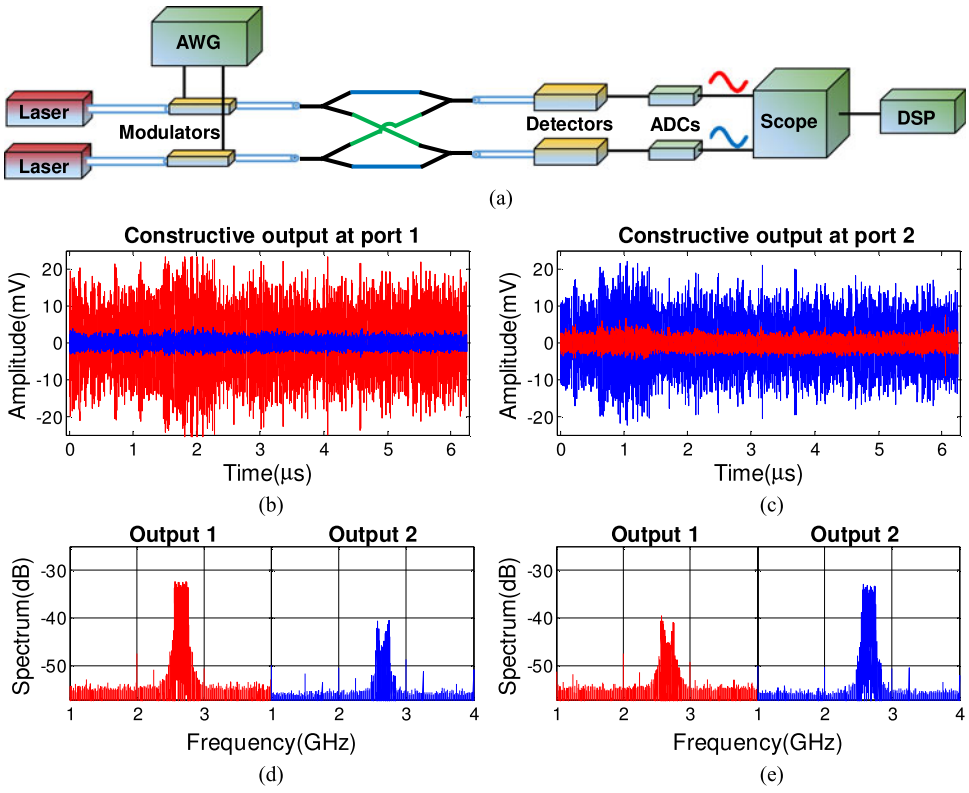

Fig. 4. Uplink demonstration. (a) Experiment setup. AWG: Arbitrary waveform generator, ADC: analog-to-digital converter, Scope: oscilloscope, DSP: digital signal processing. (b)(c) Waveforms of two output ports when the constructive output is at port 1 or 2, respectively. (d)(e) Corresponding spectrums. Red and blue curves are for output port 1 and 2, respectively.

elements have the desired phase ramp. A 200 MBaud 64-quadrature amplitude modulation (QAM) signal modulated onto a 2.5 GHz microwave carrier was generated using an arbitrary waveform generator (AWG). The operating wavelength of the laser is 1312 nm, so the chromatic dispersion (CD) is negligibly small. The constellation of the 64-QAM signal at one of the outputs is shown in Fig. 3(b); the constellation at the other port is nearly identical. The calculated error vector magnitude (EVM) for each output port of the Butler matrix is less than 2%, which is close to the back-to-back EVM of approximately 1.5%.

To characterize the relative phase between the RF signals, S_1 and S_2, at the two output ports of the Butler matrix, the cross correlation between S_1 and S_2

$$C_{12}(\tau) = \int S_1^*(t) S_2(t-\tau) dt. \tag{4}$$

is calculated. The magnitudes of the cross correlation $|C_{12}(\tau)|$ are shown in Fig. 3(c) and (d), for the signal being launched into the first and the second input ports, respectively. The phase difference between successive peaks is 180°. The highest peak appears at roughly 90° to the left of the zero delay in Fig. 3(c), which means that the phase of S_2 is 90° ahead of S_1. Similarly, the phase of S_2 is 90° behind S_1 in Fig. 3(d). So when the signal goes into different input port of the Butler matrix, there would be a $\pm 90°$ relative phase difference between the detected RF signals, as expected.

Fig. 4 shows experiment setup for uplink demonstration as well as the output RF waveforms in the time domain and their spectra at the two output ports. In Fig. 4(b)–(e), the red and blue curves are for output port 1 and 2, respectively. When the input RF signals have a $+90°$ phase difference, the constructive output port 1 has much larger RF signal compared with the destructive output port 2 as

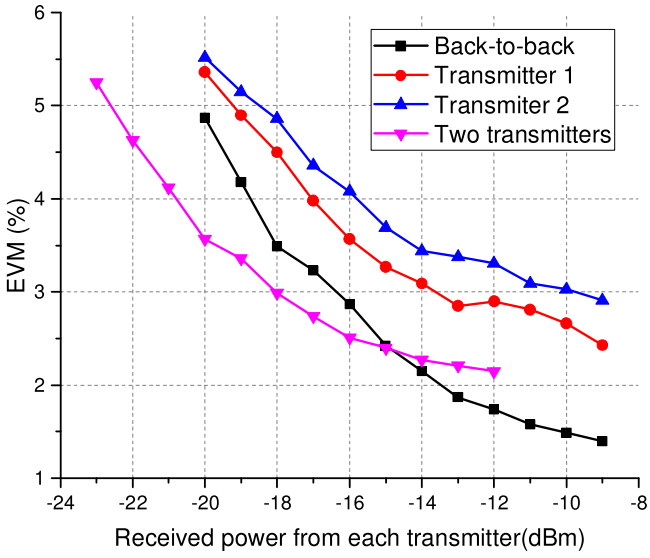

Fig. 5. EVM vs. received power from each transmitter, for uplink transmission at the constructive output port.

shown in Fig. 4(b) and (d). When there is a -90° phase difference, the destructive output port 1 has much smaller RF signal compared with the constructive output port 2 as shown in Fig. 4(c) and (e). The discrimination in carrier-to-noise ratio between the constructive and destructive ports is about 10 dB, signifying that the main power of the received signal indeed arrives at one of the desired output ports. Fourier transforms are also calculated for two outputs as shown in Fig. 4(d) and (e). For instance, in Fig. 4(d), the spectrum of the first output has the flat top, while the spectrum of the second output has smaller amplitude and the triangular dip in the center. These spectra verify that, in the uplink demonstration of the Butler matrix, constructive RF signal would appear at one output port while destructive RF signal would appear at another output port. The dip in the destructive spectrum reveals that the Butler matrix is RF frequency dependent. Nevertheless, the minimum extinction ratio at the edge of the 200 MHz bandwidth is larger than 7 dB, and more than 10 dB for most part of the 200 MHz bandwidth.

The EVMs as functions of the received power from each transmitter were measured for back-to-back transmission (no Butler matrix), only one transmitter (transmitter 1 or transmitter 2), and at the constructive port for both transmitters, respectively, as shown in Fig. 5. Comparing the EVMs between back-to-back transmission using only one transmitter, the EMV penalty for the Butler matrix network is about 1–1.5% at high received power, and below 1% at lower received power. When both transmitters are turned on, contributions from both transmitters to the amplitude of the RF signal at the constructive port add coherently. In the meantime, noises from the two transmission links add up incoherently. As a result, at low received powers, the EVM measured at the constructive port when both transmitters are turned on is reduced by a factor of approximately $\sqrt{2}$, clearly indicating the performance enhancement due to constructive beamforming. The effect of constructive beamforming is expected to be further enhanced when more beams are used.

4. Extending to Large-Scale Optical Butler Matrix

To support 5G with massive MIMO, beamforming techniques must be scalable to very large phased arrays. For the Butler matrix design of size $N \times N$, shown in Fig. 1, $\frac{N}{2}\log_2 N$ hybrid couplers and $\frac{N}{2}(\log_2 N - 1)$ phase shifters are required. This super-linear scaling in component account presents a serious obstacle for future commercial applications.

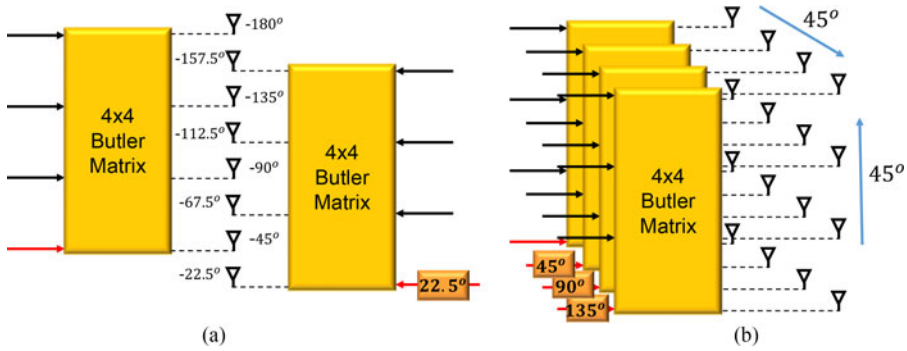

Fig. 6. Cascade of small-size Butler matrix networks. (a) One dimensional cascade. (b) Two dimensional cascade.

To reduce the component count of the Butler matrix, small-size Butler matrices can be cascaded to form large-scale Butler matrices. As shown in Fig. 6(a), cascading two 4×4 Butler matrices can form an 8×8 Butler matrix. In such a cascaded structure, the number of hybrids required is $2 \times \frac{4}{2}\log_2 4 = 8$ where an 8×8 Butler matrix requires $\frac{8}{2}\log_2 8 = 12$ hybrids. If M $N \times N$ Butler matrices are cascaded, the number of components required would be reduced by $NM\log_2 M - M + 1$, compared with a $NM \times NM$ Butler matrix. Furthermore, Butler matrices can be cascaded to form two-dimensional beamforming as shown in Fig. 6(b) where four 4×4 Butler matrices are arranged to support a 4×4 phased antenna array.

Photonic integrated circuit (PIC) may be a promising method to fabricate these large-scale RoF Butler matrixes, especially for higher RF carrier frequency. At MMW frequencies, the length of the delay line to achieve phase control can be reduced, which makes it more possible to fabricate it on PICs. In addition, higher RF carrier frequencies can also relieve the frequency squint phenomenon.

5. Conclusions and Discussions

Massive MIMO based multi-user beamforming is an important technique in future 5G wireless systems. The complexity and cost of phased antenna array networks can be an obstacle. In this work, we propose an optical implementation of the Butler matrix. With simple passive optical components and low-cost IMDD optical transceivers, hardware-efficient multi-user beamforming can be achieved. With optical routing elements, the number of signal streams connected to the baseband unit depends on the number of users, rather than the number of antenna elements. We demonstrated the 2×2 optical Butler matrix implementation for both downlink and uplink. In addition, methods for extending to larger-scale optical Butler matrix are proposed. An important component, which have not been discussed so far, for large-scale RoF Butler matrix is the optical switch. Spatial light modulators (SLMs) or digital micro-mirror devices (DMDs) demonstrated previously [17]–[19] can provide the size and speed required for current applications. In addition, waveguide switches can potentially be integrated with couplers and delay lines [20].

The 10 dB extinction ratio at the center frequency is relatively low, mainly because the signal power from each transmitter is not exactly the same due to the power variance of transmitters and the imperfect power splitting of fiber couplers, as well as mismatch between the two path lengths. However, the PIC technology should be able to significantly reduce these two imperfections. In addition, when more beams are used, the extinction ratio can be also improved due to stronger destructive interference and higher tolerance to beam nonuniformities.

When these Butler matrices are cascaded, the frequency-dependent extinction ratio would degrade, especially when the exact center frequency of each matrix differs from each other. Again, the PIC technology would alleviate this problem due to its high fabrication accuracy. The main benefit

of beamforming for MMW systems considered here is power efficiency. In this vein, even a low 6 dB extinction ratio would yield a 60% improvement in power efficiency.

References

[1] J. G. Andrews *et al.*, "What will 5G be?," *IEEE J. Sel. Area Commun.*, vol. 32, no. 6, pp. 1065–1082, Jun. 2014.
[2] A. Gupta and R. K. Jha, "A survey of 5G network: Architecture and emerging technologies," *IEEE Access*, vol. 3, pp. 1206–1232, 2015.
[3] T. S. Rappaport *et al.*, "Millimeter wave mobile communications for 5G cellular: It will work!" *IEEE Access*, vol. 1, pp. 335–349, 2013.
[4] E. Torkildson, B. Ananthasubramaniam, U. Madhow, and M. Rodwell, "Millimeter-wave MIMO: Wireless links at optical speeds," in *Proc. 44th Allerton Conf. Communic., Control Comput.*, 2006, pp. 1–9.
[5] M. Matthaiou, G. K. Karagiannidis, E. G. Larsson, T. L. Marzetta, and R. Schober, "Guest editorial: Large-scale multiple antenna wireless systems," *IEEE J. Sel. Area Commun.*, vol. 31, no. 2, pp. 113–116, Feb. 2013.
[6] J. Capmany and D. Novak, "Microwave photonics combines two worlds," *Nature Photon.*, vol. 1, no. 6, pp. 319–330, 2007.
[7] J. Yao, "Microwave photonics," *J. Lightw. Technol.*, vol. 27, no. 3, pp. 314–335, Feb. 2009.
[8] I. Aldaya, G. Campuzano, G. Castañón, and A. Aragón-Zavala, "A tutorial on optical feeding of millimeter-wave phased array antennas for communication applications," *Int. J. Antennas Propag.*, vol. 2015, 2015, Art. no. 264812.
[9] X. Liu and F. Effenberger, "Emerging optical access network technologies for 5G Wireless," *J. Opt. Commun. Netw.*, vol. 8, no. 12, pp. B70–B79, 2016.
[10] J. Corral, J. Marti, J. Fuster, and R. Laming, "True time-delay scheme for feeding optically controlled phased-array antennas using chirped-fiber gratings," *IEEE Photon. Technol. Lett.*, vol. 9, no. 11, pp. 1529–1531, Nov. 1997.
[11] Z. Cao, N. Tessema, X. Leijtens, F. Soares, and T. Koonen, "Beam steered millimeter-wave fiber-wireless system for 5G indoor coverage," in *Proc. Opt. Fiber Commun. Conf.*, 2016, Paper TU2B.1.
[12] S. Shi *et al.*, "Conformal wideband optically addressed transmitting phased array with photonic receiver," *J. Lightw. Technol.*, vol. 32, no. 20, pp. 3468–3477, Oct. 2014.
[13] C.-C. Chang, R.-H. Lee, and T.-Y. Shih, "Design of a beam switching/steering butler matrix for phased array system," *IEEE Trans. Antennas. Propag.*, vol. 58, no. 2, pp. 367–374, Feb. 2010.
[14] J. T. Gallo and R. DeSalvo, "Experimental demonstration of optical guided-wave butler matrices," *IEEE Trans. Microw. Theory Techn.*, vol. 45, no. 8, pp. 1501–1507, Aug. 1997.
[15] W. Charczenko, M. R. Surette, P. J. Matthews, H. Klotz, and A. R. Mickelson, "Integrated optical Butler matrix for beam forming in phased-array antennas," in *OE/LASE'90*, 14–19 Jan. 1990, pp. 196–206.
[16] D. Madrid, B. Vidal, A. Martinez, V. Polo, J. L. Corral, and J. Marti, "A novel 2N beams heterodyne optical beamforming architecture based on NxN optical Butler matrices," in *Proc. IEEE MTT-S Int. Microw. Symp. Dig.*, 2002, pp. 1945–1948.
[17] B. Lynn *et al.*, "Design and preliminary implementation of an N $\times$ N diffractive all-optical fiber optic switch," *J. Lightw. Technol.*, vol. 31, no. 24, pp. 4016–4021, Dec. 2013.
[18] P.-A. Blanche, B. Lynn, A. Miles, J. Wissinger, R. Norwood, and N. Peyghambarian, "Fast Non-blocking N $\times$ N optical switch using diffractive MOEMS," in *Proc. Opt. Fiber Commun. Conf.*, 2015, Paper Tu3D. 4.
[19] M. Mizukami *et al.*, "128 $\times$ 128 3D-MEMS optical switch module with simultaneous optical paths connection for optical cross-connect systems," in *Proc. Int. Conf. Photon. Switching*, 2009, pp. 1–2.
[20] K. Nashimoto, D. Kudzuma, and H. Han, "Nano-second response, polarization insensitive and low-power consumption PLZT 4 $\times$ 4 matrix optical switch," in *Proc. Opt. Fiber Commun. Conf. Expo., Nat. Fiber Optic Eng. Conf.*, 2011, pp. 1–3.